The Astrophysical Journal Letters, 736:L28 (5pp), 2011 August 1 doi:10.1088/2041-8205/736/2/L28

PROBING POPULATION III STARS IN GALAXY IOK-1 AT $z = 6.96$ THROUGH He II EMISSION

Zheng Cai[1], Xiaohui Fan[1], Linhua Jiang[1], Fuyan Bian[1], Ian McGreer[1], Romeel Davé[1], Eiichi Egami[1], Ann Zabludoff[1], Yujin Yang[2], and S. Peng Oh[3]
[1] Steward Observatory, University of Arizona, Tucson, AZ 85721, USA; caiz@email.arizona.edu
[2] Max-Planck-Institut für Astronomie, Königstuhl 17, D-69117, Heidelberg, Germany
[3] Department of Physics, University of California, Santa Barbara, CA 93106, USA
Received 2010 November 14; accepted 2011 May 27; published 2011 July 7

ABSTRACT

The He II λ1640 emission line has been suggested as a direct probe of Population III (Pop III) stars at high redshift, since it can arise from highly energetic ionizing photons associated with hot, metal-free stars. We use the *Hubble Space Telescope* WFC3/F130N IR narrowband filter to probe He II λ1640 emission in galaxy IOK-1 at $z = 6.96$. The sensitivity of this measurement is $\gtrsim 5\times$ deeper than for previous measurements. From this deep narrowband imaging, combined with broadband observations in the F125W and F160W filters, we find the He II flux to be $(1.2 \pm 1.0) \times 10^{-18}$ erg s^{-1} cm^{-2}, corresponding to a 1σ upper limit on the Pop III star formation rate (SFR) of $\sim 0.5\, M_{\odot}\, \mathrm{yr}^{-1}$ for the case of a Salpeter initial mass function (IMF) with $50 \lesssim M/M_{\odot} \lesssim 1000$ and mass loss. Given that the broadband measurements can be fit with a UV-continuum spectral flux density of $\sim 4.85 \times 10^{-10} \times \lambda^{-2.46}$ erg s^{-1} cm^{-2} Å^{-1}, which corresponds to an overall SFR of $\sim 16^{+2.6}_{-2.6}\, M_{\odot}\, \mathrm{yr}^{-1}$, massive Pop III stars represent $\lesssim 6\%$ of the total star formation. This measurement places the strongest limit yet on metal-free star formation at high redshift, although the exact conversion from He II luminosity to Pop III SFR is highly uncertain due to the unknown IMF, stellar evolution, and photoionization effects. Although we have not detected He II λ1640 at more than the 1.2σ level, our work suggests that a $\gtrsim 3\sigma$ level detection is possible with the *James Webb Space Telescope*.

Key words: dark ages, reionization, first stars – galaxies: high-redshift – galaxies: photometry

1. INTRODUCTION

The first stars, i.e., Population III (Pop III) stars with zero metallicity, are likely to be very massive due to inefficient cooling and the large Jeans mass in the early universe (Abel et al. 2002; Yoshida et al. 2006). Massive Pop III stars are probably key contributors both of the ionization photons that caused cosmic reionization and to the early phases of cosmic chemical evolution (Whalen et al. 2008; Mackey et al. 2003; Bromm et al. 2003). Although recent observations have provided major breakthroughs in understanding the universe at $z \gtrsim 7$ (e.g., Bouwens et al. 2010a; Yan et al. 2011), detection of high-redshift galaxies that contain Pop III stars remains a major challenge observationally. Indirect constraints on Pop III stars come from mapping the reionization history (Fan et al. 2006) or from studying the chemical evolution and the enrichment history through the observation of extremely metal-poor stars and hyper metal-poor stars (Beers & Christlieb 2005; Bessel et al. 2004). There are still no direct detections of high-redshift galaxies hosting star formation in zero metallicity gas.

Models show that Pop III stars are considerably hotter than present-day stars, for a given stellar mass (e.g., Johnson 2010; Bromm et al. 2003). Emission of ionizing radiation, specifically photons with energies above 54.4 eV that ionize He II, is enhanced by the high surface temperature photospheres of Pop III stars. He II λ1640 has long been suggested as a direct probe of Pop III stars (Tumlinson & Shull 2000; Oh 2001; Schaerer 2002). He II λ1640 emission is also relatively easy to model compared to resonance lines such as Lyα or He II λ304. The optical depth to He II λ1640 is small in almost all circumstances, so it does not suffer the radiative transfer effects that complicate the interpretation of Lyα flux in high-redshift galaxies (Schaerer 2003). In addition, it does not suffer from intergalactic medium (IGM) Gunn–Peterson absorption as Lyα does (Tumlinson & Shull 2000).

How can He II λ1640 emission from star formation in zero metallicity gas be distinguished from other sources? Calculations show that the He II λ1640 emission in a metal-poor stellar population with metallicity as low as $Z \sim 10^{-3}$ is still $<10^{-3}$ times lower than that in a population formed in zero metallicity gas (Tumlinson et al. 2003; Schaerer 2003). It is also known that nebular He II λ4686 was detected in a fairly large fraction of metal-poor H II regions (e.g., Skillman & Kennicutt 1993). The follow-up observations and theoretical investigations suggest that Wolf–Rayet (W-R) stars are responsible for this nebular He II emission (de Mello et al. 1998), but the hardness of this emission is more than one order of magnitude weaker than that originated by massive Pop III stars (Schaerer 2003; Jimenez & Haiman 2006). Also, the He II λ1640 equivalent width of massive Pop III stars could be a factor of two larger than that of the typical active galactic nucleus (AGN; Prescott et al. 2009; Elvis et al. 1994).

A number of studies have been carried out to search for He II emission in high-redshift galaxies at $4 < z < 6.6$. Dawson et al. (2004), Ouchi et al. (2008), and Nagao et al. (2005) searched for He II λ1640 in either stacked or individual spectra of Lyα-emitting galaxies. Nagao et al. (2008) carried out a survey for Lyα–He II emitters using a combination of intermediate and narrowband filters in the optical window. But these observations so far have yielded only nondetections, constraining the massive Pop III star formation rate (hereafter $\mathrm{SFR_{PopIII}}$) to a few $M_{\odot}\, \mathrm{yr}^{-1}$, usually a few tenths of the overall SFR in these galaxies. Yet Jimenez & Haiman (2006) predict $\mathrm{SFR_{PopIII}}$ still to be significant at $z \sim 3$–5. Even stronger metal-free star formation is expected at higher redshifts, due to less chemical feedback from Pop III stars after

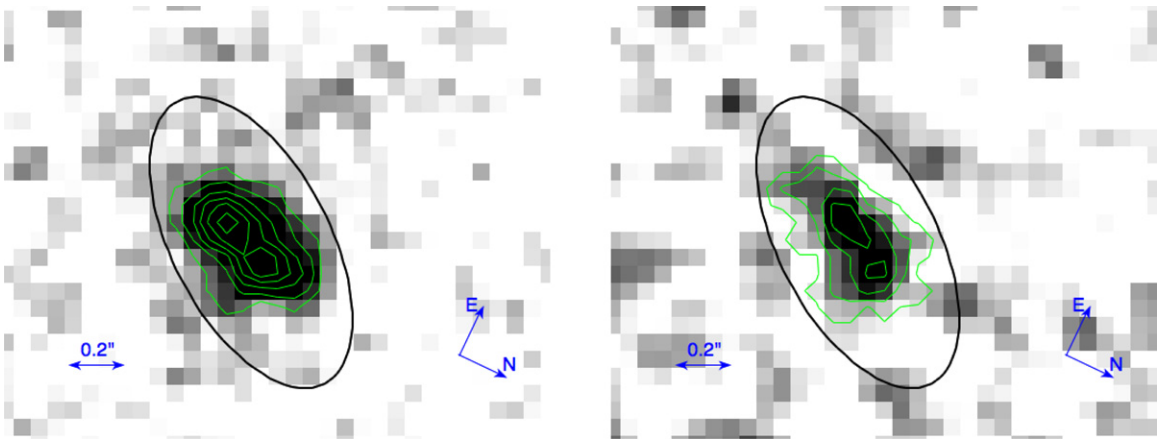

Figure 1. High-resolution images of galaxy IOK-1 in the F125W (left) and the F130N (right) bands, with contours spaced by 1.4 sky rms for the F125W image and 1 sky rms for the F130N image. The black elliptical aperture is determined by the F130N image. IOK-1 is clearly resolved into two components separated by $\sim$0.″2. Photometric analysis of the F130N image reveals a flux density excess of 1.2σ.

their initial burst. However, at $z > 7$, He II is in the J band, making ground-based observations extremely challenging. Due to its large field of view, high throughput, and low background, the new IR channel of the Wide Field Camera 3 (WFC 3) on the *Hubble Space Telescope* (*HST*) is the most powerful tool for detecting galaxies at $z \gtrsim 7$ and for studying galaxy evolution at the end of cosmic reionization.

In this Letter, we report the strongest upper limit yet on the contribution of Pop III stars in high-redshift galaxies, using deep narrowband imaging of galaxy IOK-1 (Iye et al. 2006) at $z = 6.96$ in the *HST*/WFC3 F130N band, which includes He II λ1640 at this redshift. We have also carried out deep observations in broad bands to measure the continuum level and UV-based total SFR. In Section 2, we discuss the observations and data reduction. Photometric results, including the limit on He II flux, are presented in Section 3. We discuss the implication of our results on Pop III star formation in IOK-1 in Section 4. Throughout this Letter, we adopt a cosmology based on the fifth year *Wilkinson Microwave Anisotropy Probe* data (Komatsu et al. 2009): $\Omega_\Lambda = 0.72$, $\Omega_m = 0.28$, $\Omega_b = 0.046$, and $H_0 = 70$ km s^{-1} Mpc^{-1}.

2. OBSERVATION AND THE DATA REDUCTION

Our target, IOK-1, was discovered in a narrowband Lyα emitter survey using the NB973 filter on the Subaru Suprime-Cam (Iye et al. 2006), which is centered on Lyα at $z \simeq 7.02$. This galaxy is spectroscopically confirmed at $z = 6.96$. IOK-1 has a total Lyα luminosity of $(1.1 \pm 0.2) \times 10^{43}$ erg s^{-1}, corresponding to an Lyα-based SFR, SFR$_{\rm Ly\alpha}$ $\sim 10 \pm 2\ M_\odot$ yr^{-1} (Iye et al. 2006).[4]

In the observed frame, the He II λ1640 emitted by IOK-1 is located at 13054 Å, which is in the passband of the WFC3 F130N narrowband filter ($\lambda_0 = 13006$ Å and FWHM = 150 Å). Resonant scattering of Lyα photons and IGM absorption of the blue wing usually systematically redshift the Lyα line center up to $\sim$ 700 km s^{-1} against the systemic velocity (e.g., Steidel et al. 2010). Given that He II will be located slightly blueward of the peak inferred from Lyα peak and have a narrower line width, we expect that the entire He II line falls securely into the most sensitive part of the F130N filter. IOK-1 was observed by *HST* WFC3 in 2010 March. Eight orbits ($\sim$20,000 s integration) were devoted to the F130N filter to measure the He II flux; we also observed this galaxy using the F125W filter for two orbits to determine the underlying continuum level and UV continuum-based SFR. A F160W band observation was also carried out (E. Egami et al. 2011, in preparation).

Table 1
SExtractor Photometry in Different Bands

Filter	Flux Density f^λ (10^{-20} erg s^{-1} cm^{-2} Å^{-1})	$m_{\rm AB}$
F130N	4.39 ± 0.68	25.42 ± 0.17
F125W	4.07 ± 0.19	25.59 ± 0.05

The F130N observations are divided into two visits, each consisting of a four-point dither sequence with one orbit per dither. During the first visit, the first two dither positions were affected by the presence of a bright ghost image very close to IOK-1. We exclude these two images from further analysis. The F125W continuum observation was a two-orbit single visit, which is divided into two identical four-point dither sequences, one per orbit. No ghost image affected the F125W observations. The individual images were reduced by WFC3-IR standard pipelines. Both the F130N and F125W images were combined using Multidrizzle (Koekemoer et al. 2002) with final_scale = 0.″06, which is 0.48 of the original pixel size, and final_pixfrac = 0.7. High-resolution images from the F130N and F125W bands are shown in Figure 1.

3. RESULTS

3.1. Photometry

Photometry is performed with SExtractor (Bertin & Arnouts 1996) using the rms map converted from the inverse variance image generated by Multidrizzle (Casertano et al. 2000). We measure the fluxes in the broadband (F125W and F160W) and the narrowband (F130N) images using the same Kron-like elliptical aperture determined from the F130N image (black elliptical aperture in Figure 1). The results are listed in Table 1. We also measure the flux in the F160W image of IOK-1 (E. Egami et al. 2011, in preparation), using the same aperture as used in the F125W and F130N images, finding a flux density of

[4] These error bars only reflect the photometric uncertainties. There are big systematic uncertainties due to Lyα radiative transfer effect, galaxy IMF, and metallicity assumptions. The SFR$_{\rm Ly\alpha}$ could change by a factor of two given these systematic uncertainties (also see Section 4).

$f^{\lambda}_{\rm F160W} = 2.44 \pm 0.14 \times 10^{-20}$ erg s^{-1} cm^{-2} Å^{-1}, corresponding to a magnitude of $m_{\rm F160W} = 25.98 \pm 0.06$. We fit the photometry by assuming a model spectrum with a power-law continuum with a dimensionless flux density $f_{\rm con} = {\rm A}(\lambda/1\,{\rm Å})^{\beta}$, where A is a constant and a narrow Gaussian for the He II emission line of flux $F_{\rm He\,II}$. The best-fit spectral energy distribution and photometry are shown in Figure 2. We find

$$f_{\rm con}(\lambda) = (4.85 \pm 0.23) \times 10^{-10} (\lambda/1\,{\rm Å})^{-2.46 \pm 0.36}, \quad (1)$$

$$F_{\rm He\,II} = (1.2 \pm 1.0) \times 10^{-18}\ {\rm erg\ s^{-1}\ cm^{-2}}. \quad (2)$$

At $z = 6.96$, this corresponds to a total He II luminosity of $L_{\rm He\,II} = F_{\rm He\,II} \times 4\pi D_{\rm L}^2 = (6.6 \pm 5.5) \times 10^{41}$ erg s^{-1}, or a 2σ upper limit of 1.11×10^{42} erg s^{-1}. This 2σ upper limit is a factor of $\gtrsim$(4–5)$\times$ deeper than previous measurements. The rest-frame equivalent width of He II is 4.2 ± 3.5 Å.[5] Our results also show that IOK-1 has a blue continuum. Bouwens et al. (2010b) studied the value of the UV-continuum slope β in the Hubble Ultra Deep Field (HUDF). For luminous $L^*_{z=3}$ galaxies (Steidel et al. 1999), $\beta \sim -2.0 \pm 0.2$. For lower luminosity 0.1 $L^*_{z=3}$ galaxies, $\beta \sim -3.0 \pm 0.2$. IOK-1 has an absolute magnitude $M_{\rm AB}(1500\,{\rm Å}) = -21.3$, comparable to $L^*_{z=3}$.

3.2. Morphology

The half-light radius $r_{1/2}$ of IOK-1, based on our SExtractor measurements (Bertin & Arnouts 1996) and corrected for WFC3 PSF broadening, is 0.″12 in F125W. This corresponds to 0.62 ± 0.04 kpc. IOK-1 is an extremely compact galaxy, consistent with the size of $L^*_{z=3}$ galaxies at $z \sim 7$ detected in the HUDF09 (Oesch et al. 2010). The observed surface brightness of IOK-1 is $\mu_J \sim 24.5$ mag arcsec^{-2}, corresponding to a surface brightness of $\mu_{\rm rest} \sim 15.5$ mag arcsec^{-2}, after $(1+z)^4$ correction for cosmological dimming. From Figure 1, it is obvious that IOK-1 consists of two components. We use GALFIT (Peng et al. 2002) to deblend the F125W continuum image, assuming an exponential profile for both components. The F125W image shows roughly equal brightness for the two components. The northwest component has an effective radius of 0.49 ± 0.04 kpc and the southeast component has an effective radius of 0.57 ± 0.03 kpc. The two components are projected about 0.″2 ($\sim$1 kpc) away from each other. More detailed discussions on the morphology are presented in E. Egami et al. (2011, in preparation). We also deblend the F130N narrowband image, which contains He II λ1640 emission. The northwest component is somewhat brighter. However, given the low signal-to-noise ratio of the data, this difference, while intriguing, is not statistically significant.

4. DISCUSSION

What limit can our observations place on the SFR$_{\rm PopIII}$ and its contribution to the overall star formation in IOK-1 at $z \sim 7$? Photoionization by AGNs or hot dense stellar winds from W-R stars (see, e.g., Shapley et al. 2003; Brinchmann et al. 2008) may contribute to He II λ1640 emission although at a lower level than metal-free stars. More importantly, massive stars with the lowest, but non-zero metallicity ($<10^{-8}$) could generate a comparable amount of He II λ1640 emission to Pop III stars (Schaerer 2003). However, here we assume that the observed He II emission originates entirely from metal-free stars. Therefore, our derived SFR$_{\rm PopIII}$ should be regarded as an upper limit. In the case of constant star formation, at equilibrium, recombination line luminosities L_l are proportional to the SFR$_{\rm PopIII}$ (Schaerer 2002), so

$$L_{\rm He\,II} = c_{1640}(1 - f_{\rm esc}) Q({\rm He^+}) \left(\frac{{\rm SFR_{PopIII}}}{M_\odot\ {\rm yr^{-1}}} \right) = L_{1640,{\rm norm}} \left(\frac{{\rm SFR_{PopIII}}}{M_\odot\ {\rm yr^{-1}}} \right), \quad (3)$$

where $L_{1640,{\rm norm}} \equiv c_{1640}(1 - f_{\rm esc}) Q({\rm He^+})$ is the theoretical He II λ1640 line luminosity normalized to SFR $= 1\ M_\odot$ yr^{-1}. c_{1640} is the He II λ1640 emission coefficient given in Table 1 of Schaerer (2003): $c_{1640} = 5.67 \times 10^{-12}$ erg for $T_e = 30k$ K, where nebular emission is calculated assuming case B recombination. $Q({\rm He^+})$ is the number of He$^+$ ionizing photons per second and $f_{\rm esc}$ represents the fraction of total ionizing radiation released into the IGM without being coupled to the ISM in the galaxy. We assume $f_{\rm esc} = 0$, as it is expected to be small among high-redshift galaxies (e.g., Gnedin et al. 2008). Schaerer (2002) calculates the total He$^+$ ionizing photon flux for a Salpeter initial mass function (IMF) with a range of lower and upper mass cutoffs and different assumptions of mass loss.

The conversion from He II λ1640 luminosity ($L_{\rm He\,II}$) to SFR$_{\rm PopIII}$ is affected by a number of uncertainties, including: (1) IMF, (2) mass loss, and (3) photoionization model. For the IMF, theoretical calculations show that the lack of efficient cooling mechanisms generally result in an extremely top-heavy IMF compared to a galactic IMF (Abel et al. 2002; Bromm & Larson 2004; Yoshida et al. 2006; O'Shea & Norman 2006). However, both the shape and mass range of such an IMF are poorly constrained. Scannapieco et al. (2006) suggest a lower mass cutoff of 0.8 $M_\odot$ based on metal abundances in Galactic halo stars. Numerical simulations suggest that stars as massive as 500 $M_\odot$ can be formed by accretion into a primordial protostar (Bromm & Larson 2004), which is generally taken as an upper

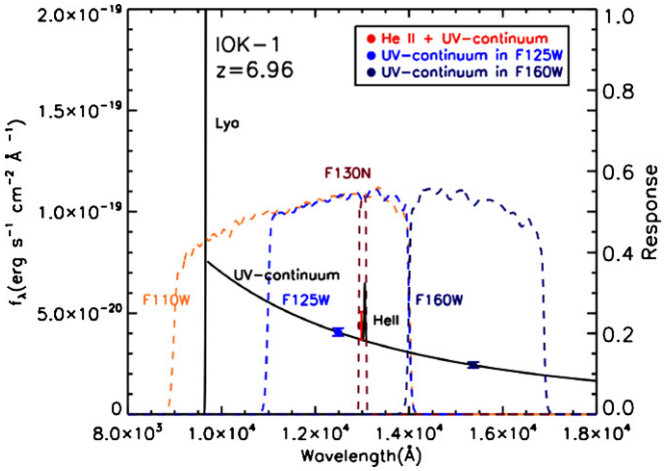

Figure 2. Best-fit spectrum (black line) of galaxy IOK-1 with the total UV continuum, as well as the Lyα and He II emission lines. The filter response curves of F125W (blue dashed line), F160W (dark blue dashed line), and F130N (brown dashed line) are plotted. In addition, photometry in three different bands is overplotted at the effective wavelength of each filter.

[5] Note that our observations could only detect He II flux stronger than 3×10^{-18} erg s^{-1} cm^{-2} at 3σ level, corresponding to an He II λ1640 equivalent width of $\sim$11 Å, which is a factor of $\gtrsim$6 larger than that of normal stellar populations in the Lyman break spectrum of stacked $z \sim 3$ galaxies (Shapley et al. 2003), and a factor of $\gtrsim$3 greater than the simulated maximum He II equivalent width generated by W-R stars (Brinchmann et al. 2008).

Table 2
Pop III Star Formation Rate

IMF (Salpeter)	Mass Loss	$L_{1640,\mathrm{norm}}$ (erg s^{-1})	$\mathrm{SFR_{PopIII}}$ ($M_\odot$ yr^{-1})
$1 \lesssim M/M_\odot \lesssim 500$	No	9.66×10^{40}	6.8 ± 4.7
$50 \lesssim M/M_\odot \lesssim 500$	No	6.01×10^{41}	1.1 ± 0.9
$1 \lesssim M/M_\odot \lesssim 500$	Yes	3.12×10^{41}	2.1 ± 1.5
$50 \lesssim M/M_\odot \lesssim 1000$	Yes	2.33×10^{42}	0.3 ± 0.2

limit in different simulations (Schaerer 2002; Scannapieco et al. 2003; Tumlinson 2006; Raiter et al. 2011). Both a Salpeter IMF (Schaerer 2003; Scannapieco et al. 2003) and a log-normal IMF (Tumlinson 2006) have been used in model calculations. Table 2 shows a factor of six difference in inferred SFR arising from different lower mass cutoffs in the Salpeter IMF.

As shown in Table 2, models with strong mass loss have a larger conversion factor $L_{1640,\mathrm{norm}}$; therefore, for the same He II luminosity, they yield a lower $\mathrm{SFR_{PopIII}}$ (Schaerer 2003). Kudritzki (2002) shows that very low metallicity stars close to the Eddington limit are subject to non-zero mass loss. Smith & Owocki (2006) argue that massive shells around luminous blue variables and so-called supernova impostors indicate that continuum-driven winds or hydrodynamic explosions dominate the mass loss of very massive stars, a claim which is insensitive to metallicity and so could apply to Pop III stars. Ekström et al. (2008) explores the effects of rotation, anisotropic mass loss, and magnetic fields on the core size of a Pop III star, pointing out that, under certain conditions, very massive stars ($140\,M_\odot < M < 260\,M_\odot$) losing mass through rotation could avoid ending their lives as pair-instability supernovae (PISNe). Whether Pop III stars end their lives as PISN or not will affect the metal ejection efficiency and hence affect the $\mathrm{SFR_{PopIII}}$. From Table 2, stronger mass loss will lower $\mathrm{SFR_{PopIII}}$ by a factor of more than three.

The derived SFR also depends on the photoionization model. Schaerer (2002) calculates nebular emission lines using standard case B recombination, in which the optical depth of the H II region is large. Equation (3) is derived under this assumption. However, for low-metallicity nebulae ionized by very hot Pop III stars, the case B predictions for line and continuum emission may have non-negligible deviations from real nebular astrophysics (Raiter et al. 2011). Therefore, the $\mathrm{SFR_{PopIII}}$ upper limits derived from Equation (3) then need to be qualitatively revised here. According to Raiter et al. (2011), for a given He II luminosity, $\mathrm{SFR_{PopIII}}$ could be a few times higher, depending on the ionizing parameters, e.g., the hydrogen number density $n(\mathrm{H})$, inner radius of the nebula r_{in}, and hydrogen ionizing photon flux $Q(\mathrm{H})$.

Our upper limit on the He II emission combined with our detection of IOK-1 in the *Spitzer* IRAC 1 and 2 bands (E. Egami et al. 2011, in preparation) suggest that IOK-1 is dominated by stars of metallicity above the critical value ($Z_{\mathrm{crit}} \sim 5\times10^{-4}\,Z_\odot$), leading to a normal IMF (e.g., Bromm & Larson 2004). Using the relation given in Madau et al. (1998), the rest-frame UV luminosity of the galaxy IOK-1 corresponds to an overall SFR $\sim 20^{+0.9}_{-0.9}\,M_\odot$ yr^{-1}. These error bars only reflect the uncertainties in the *J*-band magnitude. The true errors are larger as the conversion from UV luminosity to overall SFR is highly and systematically uncertain. In this conversion, Madau et al. (1998) assume solar metallicity; lower metallicities down to 0.0004 could lower the SFR by a factor of two (Schaerer 2003). Furthermore, the conversion assumes a Salpeter IMF with mass ranging from 0.1 to 125 $M_\odot$, whereas assuming a Scalo IMF would double the derived overall SFR. The UV-based overall SFR which should be less obscured is somewhat higher than that based on the Lyα emission line ($\sim 10 \pm 2\ M_\odot$ yr^{-1}; Iye et al. 2006), but consistent given the uncertainties in both the stellar population models and the Lyα radiative transfer effects.

The conversion of UV luminosity to an overall SFR above assumes a conversion factor between UV luminosity and SFR for Pop I and Pop II stellar populations, without correcting for Pop III stars with a top-heavy IMF. Using the fiducial Pop III Salpeter IMF of 50–500 $M_\odot$ and no mass loss, we find that our derived upper limit of 2.0 $M_\odot$ yr^{-1} for $\mathrm{SFR_{PopIII}}$ corresponds to an upper limit of 1.2×10^{-20} erg s^{-1} cm^{-2} Å^{-1} in F125W flux density. Note that the observed flux density is $(4.07 \pm 0.19) \times 10^{-20}$ erg s^{-1} cm^{-2} Å^{-1}. After correcting for the UV luminosity contributed by Pop III stars, the overall SFR is $\sim 16^{+2.6}_{-2.6}\,M_\odot$ yr^{-1}. (As stated previously, this result could change a factor of two given the systematic uncertainties associated with the IMF and metallicity assumptions.) Thus, IOK-1 is not dominated by very massive Pop III stars. It should be noted that low-mass metal-free stars do not produce an appreciable amount of He II λ1640 emission. Therefore, our observations only constrain the amount of high-mass Pop III star formation in the galaxy and cannot be used to rule out the existence of low-mass, low surface temperature Pop III stars (although, as discussed in Section 4, most theoretical calculations favor a top-heavy IMF for Pop III). Trenti & Stiavelli (2009) show that the fraction of Pop III stars $f_{\mathrm{III}}(z)$ per dark matter halo at $z \sim 10$ is only a few thousandths. Davé et al. (2006) and Tumlinson (2006) also suggest that $f_{\mathrm{III}}(z)$ in halos at $z \sim 7$ is small: $\lesssim$1%. Taking into account the systemic uncertainties in the UV-based overall SFR, our observations indicate that the galaxy IOK-1 cannot be dominated by Pop III stars with very top heavy IMFs. For example, for a Salpeter IMF with $50 \lesssim M/M_\odot \lesssim 500$ and no mass loss, the ratio of $\mathrm{SFR_{PopIII}}$ to the overall SFR is $\lesssim 25\%$. For a Salpeter IMF with $50 \lesssim M/M_\odot \lesssim 1000$ and mass loss, the ratio is $\lesssim$6%.

Our deep *HST* narrowband imaging places the strongest constraint yet on the $\mathrm{SFR_{PopIII}}$ in high-redshift galaxies. Although we have not detected the He II emission line in IOK-1 at more than 1.2σ, this limit suggests that detection of He II emission from Pop III stars may be already within the reach of current facilities. Future facilities, especially the *James Webb Space Telescope* and GSMT, will be likely to probe down to the $\gtrsim 3\sigma$ level and directly detect the signatures of the earliest star formation in the universe.

We thank the anonymous referee for insightful comments which have significantly improved the Letter. We thank Stefano Casertano, Daniel Schaerer, and Haojing Yan for useful discussions. Support for this work was provided by NASA through grant HST-GO-11587 from the Space Telescope Science Institute, which is operated by AURA, Inc., under NASA contract NAS5-26555. Z.C., X.F., L.J., F.B., and I.M. acknowledge support from NSF grant AST 08-06861 and a David and Lucile Packard Fellowship. A.I.Z. acknowledges support from the NSF through grant AST-0908280 and from NASA through grant NNX10AD47G.

REFERENCES

Abel, T., Bryan, G. L., & Norman, M. L. 2002, Science, 295, 93
Beers, T. C., & Christlieb, N. 2005, ARA&A, 43, 531

Bertin, E., & Arnouts, S. 1996, A&AS, 117, 393
Bessel, M. S., Chrislieb, N., & Gustafsson, B. 2004, ApJ, 612, L61
Bouwens, R. J., et al. 2010a, ApJ, 709, L133
Bouwens, R. J., et al. 2010b, ApJ, 708, L69
Brinchmann, J., Pettini, M., & Charlot, S. 2008, MNRAS, 385, 769
Bromm, V., & Larson, R. B. 2004, A&A, 42, 79
Bromm, V., Yoshida, N., & Hernquist, L. 2003, ApJ, 596, L135
Casertano, S., et al. 2000, AJ, 120, 2747
Davé, R., Finlator, K., & Oppenheimer, B. D. 2006, MNRAS, 370, 273
Dawson, S., Rhoads, J., & Malhotra, S. 2004, ApJ, 617, 707
de Mello, D. F., Schaerer, D., Heldmann, J., & Leitherer, C. 1998, ApJ, 507, 199
Ekström, S., Meynet, G., Hirschi, R., & Maeder, A. 2008, in IAU Symp. 255, Low-metallicity Star Formation: From the First Stars to Dwarf Galaxies (Cambridge: Cambridge Univ. Press), 194
Elvis, M., et al. 1994, ApJS, 95, 1
Fan, X., Carilli, C. L., & Keating, B. 2006, ARA&A, 44, 415
Gnedin, N. Y., Kravtsov, A. V., & Chen, H. 2008, ApJ, 672, 765
Iye, M., et al. 2006, Nature, 443, 186
Jimenez, R., & Haiman, Z. 2006, Nature, 440, 501
Johnson, J. L. 2010, MNRAS, 404, 1425
Koekemoer, A. M., Fruchter, A. S., Hook, R. N., & Hack, W. 2002, in The 2002 HST Calibration Workshop: Hubble after the Installation of the ACS and the NICMOS Cooling System, ed. S. Arribas, A. Koekemoer, & B. Whitmore (Baltimore, MD: Space Telescope Science Institute), 337
Komatsu, E., et al. 2009, ApJS, 540, 330
Kudritzki, R. P. 2002, ApJ, 577, 389
Mackey, J., Bromm, V., & Hernquist, L. 2003, ApJ, 586, 1
Madau, P., Pozzetti, L., & Dickinson, M. 1998, ApJ, 498, 106
Nagao, T., Maiolino, R., & Marconi, A. 2005, ApJ, 631, L5
Nagao, T., Sasaki, S. S., & Maiolino, R. 2008, ApJ, 680, 100
Oesch, P. A., et al. 2010, ApJ, 709, L21
Oh, S. P. 2001, ApJ, 553, 499
O'Shea, B. W., & Norman, M. L. 2006, ApJ, 648, 31
Ouchi, M., Shimasaku, K., & Akiyama, M. 2008, ApJS, 176, 301
Peng, C. Y., Ho, L. C., Impey, C. D., & Rix, H. 2002, AJ, 124, 266
Prescott, M. K. M., Dey, A., & Jannuzi, B. T. 2009, ApJ, 702, 554
Raiter, A., Schaerer, D., & Fosbury, R. A. E. 2011, A&A, 523, A64
Scannapieco, E., Kawata, D., Brook, C. B., Schneider, R., Ferrara, A., & Gibson, B. K. 2006, ApJ, 653, 285
Scannapieco, E., Schneider, R., & Ferrara, A. 2003, ApJ, 589, 35
Schaerer, D. 2002, A&A, 382, 28
Schaerer, D. 2003, A&A, 397, 527
Shapley, A. E., Steidel, C. C., Pettini, M., & Adelberger, K. L. 2003, ApJ, 588, 65
Skillman, E. D., & Kennicutt, R. C., Jr. 1993, ApJ, 411, 655
Smith, N., & Owocki, S. P. 2006, ApJ, 645, L45
Steidel, C. C., Adelberger, K. L., Giavalisco, M., Dickinson, M., & Pettini, M. 1999, ApJ, 519, 1
Steidel, C. C., Erb, D. K., Shapley, A. E., Pettini, M., Reddy, N., Bogosavljević, M., Rudie, G. C., & Rakic, O. 2010, ApJ, 717, 289
Trenti, M., & Stiavelli, M. 2009, ApJ, 694, 879
Tumlinson, J. 2006, ApJ, 641, 1
Tumlinson, J., Michael, S. J., & Venkatesan, A. 2003, ApJ, 584, 608
Tumlinson, J., & Shull, J. M. 2000, ApJ, 528, L65
Whalen, D., O'Shea, B. W., Smidt, J., & Norman, M. L. 2008, ApJ, 679, 925
Yan, H., et al. 2011, ApJ, 728, L22
Yoshida, N., Omukai, K., Hernquist, L., & Abel, T. 2006, ApJ, 652, 6